

Comparison of Changes in Gross and Microscopic Morphometry and Function of the Olfactory System in Rabbits Administered Single Human Equivalent Doses of Vinblastine Sulfate and Docetaxel

Boniface Mwanzia Kavoi¹

¹Department of Veterinary Anatomy and Physiology, Faculty of Veterinary Medicine, University of Nairobi, Riverside Drive, P.O., Nairobi, Kenya

Disclose and conflicts of interest: none to be declared by all authors

ABSTRACT

Introduction: vinblastine (VBS) and docetaxel (DCT), classified as vinca alkaloids and taxanes respectively, are microtubule-targeted drugs (MTTDs) used in cancer chemotherapy. These drugs act by disrupting microtubule dynamics in highly proliferative cells, including those of olfactory system (OS), through different mechanisms. Data on differences in morphometric and functional changes produced on the OS by these drugs remain insufficient.

Materials and Methods: Single systemic human equivalent doses of VBS and DCT were administered to adult rabbits. At post-exposure day 10, the olfactory mucosa (OM) and olfactory brain components (OBCs) were analyzed, quantitatively, for gross, microscopic and functional alterations.

Results: relative to controls, respective decrease in volumes (%) for olfactory bulb (OB), OBCs and whole brain (WB) were 12.5, 10.53 & 11.92 for VBS and 25.0, 15.79 & 18.95 for DCT. Respectively, OB, OBC and cerebral hemisphere (CH) lengths decreased by 4.01, 11.8 & 8.66% for VBS and 5.90, 14.43 & 12.24% for DCT whereas OB and CH breadths decreased by 1.73 & 6.24% for VBS and 3.03 & 8.99% for DCT. Respective values for OM epithelial thickness, olfactory receptor neuron (ORN) axon bundle diameter, ORN packing density, and cilia number per ORN decreased by 7.03, 26.8, 9.6 & 16.5% for VBS and 23.04, 52.6, 63.1 & 50.0% for DCT. Olfactory sensitivity decreased 5.4-fold and 7.0-fold for VBS and DCT respectively.

Conclusion: single parenteral doses of VBS and DCT impact negatively on the OS by altering its quantitative structure and function in a manner that is more pronounced in the latter drug.

Keywords: Docetaxel; Vinblastine; Morphometry; Olfactory system; Rabbit.

Introduction

The olfactory system (OS) processes information about the identity, concentration and quality of odors, playing critical roles in feeding (food detection, identification and regulation of appetite), reproduction (mating and mother-infant bonding) and avoidance of danger^{1,2,3}. Data on the basic structure and function of the mammalian OS, including the olfactory mucosa (OM) and the olfactory bulb (OB), are available in the literature^{4,5,6}. Odorants interact with olfactory receptor neurons (ORNs) in the epithelium of the OM in the nasal cavity^{7,8}. Axons arising from the ORNs fasciculate in the OM lamina propria to form axon bundles before projecting to the OB to synapse with second order neurons (mitral and tufted cells), which in turn project to various regions of the olfactory cortex^{9,10}. The olfactory tract is formed by a bundle of nerve fibers that connect the OB with the olfactory cortex while olfactory striae are the ridges formed, laterally and medially, when fiber bundles of the olfactory tract split on reaching the olfactory areas of the cerebral cortex^{11,12}.

Neurogenesis continues throughout life in specific areas of nervous system including the hippocampus, OB and OM epithelium, with the latter two structures being of particular interest as they contribute new neurons to both ends of a first-level circuit governing olfactory perception¹³. The OS is in direct contact with the external environment putting it at risk of injury by environmental agents including toxicants and pathogens^{14,15}. These agents induce inflammation of the nasal cavity resulting in alteration of the normal OM structure and reduction in ORN numbers¹⁴. Inflammation triggered by noxious agents on the OM also disrupts the anatomy and homeostatic function of the OB, causing reduction in its size and dysregulation of intrabulbar circuits¹⁶. Cancer chemotherapy utilizes a wide range of parenterally administered drugs, majority of which are anti-proliferative. Although some degree of specificity in the action of these drugs to cancer cells come from the inability of many cancer cells to repair DNA damage¹⁷, they have the potential to cause injury to normal tissues characterized high cell turnover such as bone marrow,

GIT lining, reticuloendothelial system, gonads, hair follicles, gustatory and olfactory epithelia^{18, 19}. In the OS, chemotherapy is associated with loss of olfactory function during and after treatment with consequent deleterious effects on the patient's nutritional intake, quality of life and overall prognosis²⁰.

Taxanes and vinca alkaloids are among the widely used group of antiproliferative drugs used in chemotherapy for many types of cancer. These drugs, also called microtubule-targeting (MTTDs) or anti-tubulin drugs, are plant-derived and act by disrupting microtubules to inhibit mitosis^{21,22}. Microtubules are made up α - and α -tubulin heterodimers that interconvert between phases of rapid growth and shrinkage and functions in maintenance of cell shape, cell motility, epithelial polarity and formation of spindle fibers, chromosome segregation, intracellular trafficking of macromolecules and organelles during cell division and formation of cilia or flagella^{21,22}. Neurons are striking examples of cells in which microtubules are essential for achieving a high degree of morphological and functional complexity²³. Indeed, biochemical similarities between filaments of the mitotic spindle and those of neuronal axons justify why neurons are vulnerably to damaging effects of MTTDs²⁴. Vinca alkaloids (e.g. VBS, vincristine, vinorelbine, vindesine and vinflunine) arrest cell division by inducing tubulin to form alternate spiral polymers that dissociate microtubules by peeling spiral protofilaments^{25,26}. Conversely, taxanes (e.g. DCT, paclitaxel and cabazitaxel) bind reversibly to microtubule polymers within microtubule lumen to enhance polymerization of tubulin^{27,28}.

Previously, experimental studies have examined the effect of MTTDs in highly proliferative tissues including lymphohematopoietic, GIT, testicular^{29,30} and cutaneous tissues³¹, with little focus on the OS. The studies by Kai and colleagues, whose scope was limited to qualitative analysis of the OM epithelium, demonstrated remarkable differences in susceptibility of the epithelium to lesions induced by MTTDs with regard to drug type, dosage and animal specie^{32,33,34,35}. In our earlier work in rabbits^{36,37}, we analyzed the effects of DCT and VBS only on the OM and from a non-comparative point of view. In an attempt to fill this knowledge gap and to generate new data, the current study compared VBS and DCT with regard to the extent to which they distort the gross, microscopic and functional integrity of the rabbit OS both in the nasal cavity (OM) and in the brain (OBCs).

Materials and Methods

Experimental Animals

This study utilized a total of forty two clinically healthy adult male New Zealand White rabbits aged 6–8 months and weighing 2.5–3.5 kg. These rabbits were purchased from commercial breeders in Njoro

Sub-county, Rift Valley, Kenya. The animals were transported to the housing facility at the Department of Veterinary Anatomy and Physiology, University of Nairobi, where they were kept in individual wire mesh cages and under conditions of 12-h light/dark cycle, ambient temperatures 23 ± 2 °C and relative humidity $55 \pm 15\%$. They were fed on standard rabbit pellets (Unga feeds Ltd, Nairobi, Kenya) and tap water was available *ad libitum*. The animals were allowed to acclimatize to the housing conditions for four weeks before starting the experiments. All protocols for the experimentation of the animals were approved by the Animal Use and Care Committee of the University of Nairobi (730/2008) and strictly adhered to the National Institutes of Health (NIH) Guide for the Care and Use of Laboratory Animals.

Animal Grouping

For this work, animals were distributed to various groups as shown Table 1. They were randomly assigned to three treatment groups (designated A, B and C) and three control groups (D, E and F) with each group having seven animals. Respectively, groups A and B animals were treated with VBS and DCT and euthanized for olfactory brain morphometry only (data on OM morphometry are available in our earlier papers^{36,37}). Group C animals were administered VBS and used for olfactory function test (data on olfactory function for DCT are also available³⁷). Groups D, E and F served as controls for olfactory function test, brain morphometry and OM morphometry respectively.

Table 1. Summary of distribution of the experimental animals into various treatment groups. Data on olfactory function for docetaxel and on olfactory mucosa (OM) morphometry for vinblastine and docetaxel are available in our earlier papers^{36,37}.

Study	OM Morphometry	Brain Morphometry	Olfactory Function Test
Controls	7	7	7
Vinblastine	-	7	7
Docetaxel	-	7	-

Administration of Test Drugs

Lyophilized formulation of VBS and DCT (Surgipharm Ltd, Nairobi, Kenya) were dissolved in physiological saline and administered to the rabbits as single human equivalent doses of 0.31 and 6.26 mg/kg, respectively, via the ear vein. In humans, VBS is administered at a dose rate of 3.7 mg/m² (0.10 mg/kg)³⁸ whereas DCT is given at 75 mg/m² (2.03 mg/kg)³⁹ and therefore the doses given to the rabbits were worked out using the formula:

Animal dose = Human dose x (Human K_m factor / Animal K_m factor)

[Where: K_m factor, body weight (kg) divided by body surface area (m²), is 37 for humans and 12 for rabbits⁴⁰]

Control animals were injected with a corresponding volume of physiological saline also through the ear vein.

Harvesting of Brains and Olfactory Mucosa

Representative groups of animals for morphometric work (VBS & DCT-treated animals for brain work and controls for OM and brain) were euthanized with lethal doses of pentobarbital sodium (200 mg/kg, intraperitoneally). For the VBS and DCT-treated animals, euthanasia was done at post-exposure day 10. Perfusion fixation of freshly euthanized animals was performed transcardially through the left ventricle with saline followed by 10% formaldehyde, after which the carcass head was detached from the rest of the body at the atlanto-axial joint using a sharp knife. Harvesting and sampling of the OM were performed as described for dogs and sheep⁴¹. Thus, the OM was obtained from the ethmoturbinates after mid-sagittal sectioning of the skull and removal of the nasal septum. This was followed by transection of the ethmoturbinates perpendicular to their long axes into anterior, middle and posterior portions from where tissue sub-segments were selected by systematic random sampling for microscopy (Figure 1). Brain harvesting was done as detailed before⁴², by skinning and stripping off the cranial and facial muscles prior to breaking the skull using a dissecting knife and a pair of thumb forceps to extract the brain (with the bulbs intact). The harvested brains and OM tissues

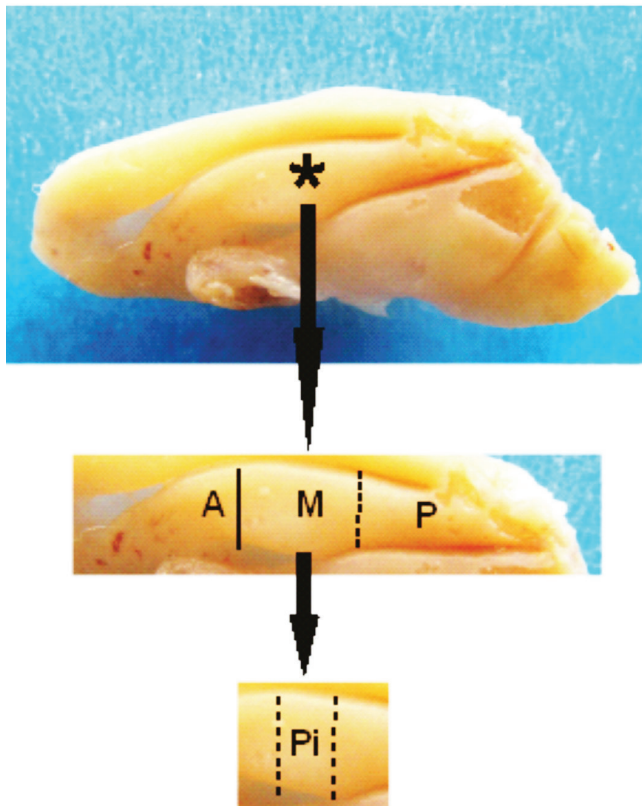


Figure 1. Macrograph of ethmoturbinates of the rabbit illustrating the steps followed in tissue sampling. Tissue blocks were obtained from anterior (A), middle (M) and posterior (P) portions of the turbinate using a sharp blade. Each of these portions was further transected into smaller pieces (Pi). For microscopic analysis, tissue pieces obtained from each of the three levels were selected by systematic random sampling.

were allowed to fix further by immersion in 10% formaldehyde for 24 hours.

Processing of the olfactory mucosa for light and scanning electron microscopy

Selected ethmoturbinate pieces were decalcified in 5% phosphate buffered EDTA⁴³, washed in distilled water and dehydrated in graded ethanol series (50, 70, 80, 90% and twice in 100%). This was followed by infiltration and embedding in paraffin wax and sectioning of the tissues in the transverse plane at 5µm using a rotary microtome (Leitz Wetzlar, Germany). Staining was then done in H&E and Masson's trichrome following routine procedures. For scanning electron microscopy (SEM), tissue pieces were dehydrated in increasing concentrations of acetone (50% to 70, 80, 90, 95, and 100% x2), critical point dried in liquid carbon dioxide, mounted on brass stubs and sputter-coated with gold-palladium complex. The sample surfaces were then viewed on a Jeol 330 or Leo 1530 SEM at 15 kV

Morphometric Analysis of the Olfactory Mucosa

Quantitative parameters of the OM were analyzed at both light microscopy and SEM levels using a graticule fitted inside the eyepiece of the microscope⁴⁴. To this end, tissue samples were randomly selected and processed from the seven animals (four for light microscopy and three for SEM) from which 10-15 histology and 8-10 SEM micrographs were prepared. In both cases, morphometric analysis was done on 30-35 test fields generated from randomly selected micrographs. The OM was analyzed for epithelial thickness and ORN axon bundle diameter at light microscopic level and for ORN packing density and cilia number per ORN knob at SEM level. All the aforementioned parameters were determined following the steps detailed in our earlier paper⁴. In brief, the thickness of OE was measured from the basement membrane to the apical surface while diameters ORN axon bundle were worked out from mean linear intercept lengths. Volume densities were estimated by point counting using an overlay of a coherent test system of points. Packing densities of ORN were estimated by counting the ORN knobs projecting from the OM epithelial surface in a millimeter square area while taking into account the forbidden line rule. In determining cilia counts/ ORN knob, the obscured cilia, which are estimated at 25%, were incorporated in the final total value.

Determination of linear dimensions and volumes of brain components

Linear measurements of the cerebral hemispheres (CHs) and olfactory brain components (OBC) [olfactory bulb (OB), olfactory tract and stria combined⁴⁵] were carried out as described for elephant shrews⁴⁵. To this end, the length and breadths of the CHs were taken (on the brain in situ) at their greatest points from the dorsal aspect of the brain. The OBCs were then

marked out for dissection and removed, en bloc, and its length determined. Thereafter, the OB was separated from the underlying olfactory tract to estimate its greatest length and breadth. The measurements were performed by two trained technicians (intra and inter-observer errors = 2-3%) using vernier calipers, thread and meter rule. The volume of the whole brain (WB) and that of the OBC were determined using Water Immersion Volumetry⁴⁶. Thus, a beaker containing sufficient amount of saline was placed on a digital weighing balance and the structure to be weighed (initially suspended from a clamp stand with a fine thread) was completely dipped in the saline, and the change in weight reading (in grams) taken to be equivalent to the volume of the structure (in cubic centimeters).

Assessment of Olfactory Function Using Hidden Cookie Test

The hidden cookie test, also known as food exploration test, food localization test or buried food pellet recovery test^{47,48}, measures the animal's natural tendency to use the olfactory cue for foraging and therefore its general ability to smell. To examine the impact of VBS administration on olfactory sensitivity in the rabbit, the test was performed in steps as described elsewhere⁴⁹: Step 1: Odor familiarization where a piece of dry cookie (made from rabbit food pellets) was put in the subject's cage for 2-3 consecutive days before the test with daily checks to confirm if the cookie had been consumed. Step 2: Food deprivation where all food was removed from the cage 18-24 hours before the test but with provision of water *ad libitum*. Step 3: Scoring the latency to find the cookie where, (i) the subject was placed in a standard cage measuring 52 cm long x 42 cm wide x 41 cm high⁵⁰ containing clean bedding and allowed to acclimate for 5-10 minutes, (ii) the subject was transferred to an open wooden box (of similar dimension as the standard cage) containing clean bedding underneath which a 5 gram piece of cookie was buried approximately 6 cm beneath the surface (Figure 2), (iii) recording was done on the latency time i.e. the time taken (in seconds) between placement of the subject rabbit in the box and grasping the cookie with its teeth. Latency scores were taken three times for each subject (using a video camera) by an experimenter blinded to the test information in all trials and positioned 2m away from the box. A deficit in olfactory ability was recorded for subjects who failed to find the cookie after 300 seconds had elapsed.

Statistical Analysis

Comparison of changes in OM and brain morphometric values between controls and treated animals were recorded as percentages. For differences in olfactory sensitivity, latency scores were compared between controls and treated animals using the Student's t-test and with graphical representation



Figure 2. A photograph of the set up used to measure latency scores in the hidden cookie test. After odor familiarization, food deprivation and acclimatization, the subject rabbit was placed in an open wooden box measuring 52cm long, 42cm wide and 41cm high and containing clean wooden shavings below which piece of cookie (5g) was buried about 6cm beneath the surface. The subject was then allowed time to locate and uncover the cookie. Latency time was recorded as the time (in seconds) between placement of the subject in the box and grasping the cookie with its teeth.

of the data. In all cases, mean values were presented together with their standard deviations (SD) and statistical significance was captured at $p < 0.05$.

Results

Table 2 contains data on linear dimensions (greatest lengths and breadths) of OB, OBC and CH in controls and in rabbits administered with VBS and DCT. Relative to controls, a decrease in linear measurements of the three structures is noted, with the degree of reduction being greater in DCT than in VBS-treated animals. Length measurements (in mm) in controls were 15.23 ± 1.36 for OB, 26.61 ± 2.11 for OBC and 36.60 ± 3.18 for CH and these decreased in VBS-treated animals by 4.01, 11.88 and 8.66% and with DCT-treatment by 5.90, 14.43 and 12.24% respectively. For the breadths, control values (in mm) were 6.92 ± 0.87 for OB and 24.36 ± 2.15 for CH and these decreased by 1.73 and 6.24% with VBS

Table 2. Mean values (\pm SD given in parenthesis) of linear measurements of the olfactory bulb (OB) alone, OB, olfactory tracts and stria combined (OBC) and cerebral hemispheres (CHs) (in mm) in controls and in vinblastine and docetaxel-treated rabbits, and their percentage decrease relative to the controls at post-exposure day 10.

Parameter	Control	Vinblastine	Docetaxel
Length OB	15.23 (1.36)	14.62 (1.13)	14.33 (1.27)
Decrease %		4.01	5.90
Breadth OB	6.92 (0.87)	6.80 (0.75)	6.71 (0.84)
Decrease %		1.73	3.03
Length OBC	26.61 (2.11)	23.45 (1.97)	22.77 (1.88)
Decrease %		11.88	14.43
Length CH	36.60 (3.18)	33.43 (2.91)	32.12 (2.67)
Decrease %		8.66	12.24
Breadth CH	24.36 (2.15)	22.84 (1.78)	22.17 (1.93)
Decrease %		6.24	8.99

treatment and by 3.03 and 8.99% with DCT treatment, respectively.

Data on volumes for OB, OBC and WB are provided in Table 3. Control values for volume (in cm³) were 0.08±0.01 for OB, 0.19 ±0.05 for OBC and 13.67±1.80 for WB. Respectively for the OB, OBC and WB, the values decreased more remarkably in DCT- treated rabbits (25.0, 15.79 & 18.95%) as compared with VBS-treated animals (12.5, 10.53 & 11.92%)

Table 3. Mean values (±SD given in parenthesis) for volumes (in cm³) of the olfactory bulb (OB) alone, OB, olfactory tract and stria combined (OBC) and whole brains (WB) for controls and for vinblastine and docetaxel- treated rabbits, and the percentage decrease in the volumes relative to the controls at post-exposure days 10.

Parameter	Control	Vinblastine	Docetaxel
Volume OB (cm ³)	0.08 (0.01)	0.07 (0.01)	0.06 (0.01)
Decrease (%)		12.5	25.0
Volume OBC (cm ³)	0.19 (0.05)	0.17 (0.05)	0.16 (0.04)
Decrease (%)		10.53	15.79
Volume WB (cm ³)	13.67 (1.8)	12.04 (1.5)	11.08 (1.4)
Decrease (%)		11.92	18.95

Differences in OM morphometric values between controls (current study) and VBS and DCT- treated animals (previous studies) are recorded in Table 4. Respectively, OM epithelial thickness (µm), ORN axon bundle diameter (µm), ORN packing density (mm⁻²× 10³) and cilia counts/ ORN knob which were 98.1±2.8, 129.6±10.3, 88.9±4.7 and 24±3 in control animals, decreased by 7.03, 26.8, 9.6 & 16.5% with VBS-treatment and by 23.04, 52.6, 63.1 and 50.0 with DCT-treatment.

In Figure 3, olfactory sensitivity scores in controls are compared with those of animals treated with

Table 4. Mean values (±SD given in parenthesis) for OM epithelial thickness, olfactory receptor neuron (ORN) axon bundle diameter (in µm), packing densities of ORNs (mm⁻² × 10³) and cilia counts per ORN in controls (current study) and in vinblastine and docetaxel-treated rabbits (previous studies), and the percentage decrease in these parameters relative controls at post-exposure day 10.

Parameter	Control (Current study)	Vinblastine (Previous study ³⁶)	Docetaxel (Previous study ³⁷)
Epithelial thickness	98.1 (2.8)	91.2 (2.9)	75.5 (4.3)
Decrease %		7.03	23.04
Axon bundle diameter	129.6 (10.3)	94.9 (12.6)	61.4 (8.9)
Decrease %		26.8	52.6
ORN packing density	88.9 (4.7)	80.4 (4.2)	32.8 (3.3)
Decrease %		9.6	63.1
Cilia number/ ORN	24 (3)	20 (2)	12 (3)
Decrease %		16.5	50.0

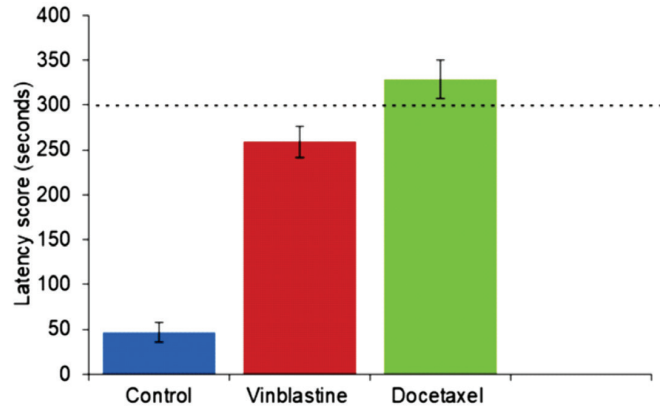


Figure 3. Mean latency scores (in seconds) of controls and of rabbits injected with vinblastine (current study) and docetaxel³⁷, and tested for olfaction sensitivity on post-exposure day 10. Relative to the controls, latency scores increased significantly in vinblastine-treated rabbits (5.4-fold), and even more markedly with docetaxel-treatment (7.0-fold) where the animals showed olfactory deficit and inability to locate and uncover the cookie, p < 0.05.

VBS (current study) and docetaxel (earlier study) at post-exposure day 10. Relative to the control value (47± 11seconds), latency scores increased significantly (p< 0.05) in VBS-treated animals (5.4-fold) and DCT treatment (7.0-fold), with the latter drug producing a deficit in olfactory function and inability to locate and uncover the hidden cookie.

Discussion

The combined perception in flavor of food by the olfactory and gustatory epithelia is an important determinant with regard to food intake and nutritional status. Although chemotherapy improves the survival of cancer patients, the drugs used cause severe side effects leading to poor nutrient intake and reduced efficacy of the anticancer treatment^{20,51}. Clinical reports on various forms of MTTDs-induced olfactory dysfunction have been presented by several authors^{52,53,54,55} with scanty details on the exact nature and magnitude of lesions associated with such dysfunctions. Further, there have been attempts to document, using different experimental models, the structural distortions produced by MTTDs on the OM^{32,33,34,35,4,37}. However, none of the studies has compared the degree of structural and functional disruptions that VBS (a vinca alkaloid) and DCT (a taxane) cause on the OS in its entirety, both grossly and microscopically. Thus, this study provides the first comprehensive comparison regarding the magnitude of macroscopic, microscopic and functional alterations that VBS and DCT produce on OS structures in the nasal cavity and the brain.

Anticancer drug VBS is a first-generation vinca alkaloid developed from Periwinkle plant (*Catharanthus roseus*)⁵⁶. This drug inhibits mitosis by aggregating tubulin to disrupt microtubule assembly and is used in treating melanoma, non-small cell lung cancer, testicular cancer, brain cancer, and Hodgkin's lymphoma^{26,57,58}. In contrast, DCT is a semisynthetic

analogue of paclitaxel derived from the bark of Pacific yew (*Taxus Brevifolia*)⁵⁹. It arrests cell replication by stabilizing GDP bound tubulin to block microtubule disassembly and is used in treating breast cancer (as first-line therapy), ovarian, prostate, lung, gastric, bladder, head and neck cancers^{60,61}. The rabbit, which is an excellent model for toxicological work⁶², was used in this study to demonstrate changes produced on the OS structure by VBS and DCT (viz. linear dimensions and volumes of OB and OBCs, thickness of OM epithelium, diameter of ORN axon bundles, density of ORN and number of cilia/ ORN) with the finding that the two drugs caused a reduction in all the above parameters but to greater extent with DCT treatment. This observation that was further confirmed by recording of latency scores for olfactory sensitivity in this study. Plausibly, these findings may be a reflection of the difference in the mechanisms of action of the two groups of drugs.

Undisrupted, the OM epithelium remains in a steady state of equilibrium between cell loss and cell replacement⁶³. With DCT and VBS treatment, cells of the rabbit OM epithelium were shown to lose their normal arrangement^{36,37}. Additionally, administration of VBS and DCT in rabbits^{36,37} or vincristine in mice³² resulted in sporadic mitotic figures at the basal region of the OM epithelium. Several intercellular adhesion systems including tight junctions are maintained by cell-cell contact and apical-basal polarity in epithelia⁶⁴. Arguably, these adhesion systems may be disrupted by MTTDs to cause the disarrangement noted in the above studies. Additionally, regenerative response to cell death after MTTD treatment is believed to be the reason for presence of mitotic figures seen in the OM epithelium³⁷. In paclitaxel-treated mice, death of OM epithelial cells was reported to occur through apoptosis with resultant epithelial atrophy³³. Apoptotic cell death and degeneration were also demonstrated in ORN axon bundles of rabbits treated with VBS and DCT^{36,37}. Notably, these qualitative changes appear to match closely with our morphometric data (of reduced OM epithelial thickness, ORN packing density and bundle diameters) where DCT presents a higher level of reduction than VBS at post-exposure day 10.

Olfactory cell cilia, which provide the sites for odor binding, are microtubule-based structures⁶⁵ and as such, they are highly prone to the disruptive effects of MTTDs. This, apparently, can be attributed to the current findings of reduced ORN packing density and

cilia number/ ORN in VBS and DCT treated rabbits and the concomitant decline in olfactory sensitivity, which was more pronounced in the DCT-treated group. Studies detailing the effects of noxious agents on the OB¹⁶ showed prolonged inflammation of the nasal cavity to result: (1) hyposmia or anosmia (2) similar consequences on the functional structure of the OB, (3) atrophy of the OB via thinning of its layers particularly the olfactory nerve layer, glomerular layer and superficial external plexiform layer and, (4) dysregulation of the connectivity between ORNs, OB projection neurons and interneurons through synaptic pruning and dendritic retraction. This may help to justify the findings of this study, whereby distortions induced by VBS and DCT in the OM are mirrored in the OB and its tracts, as evidenced by reduction in their size and volume.

Conclusion

Overall, results of this work show that systemic administration of single human equivalent doses of anticancer drugs VBS (a vinca alkaloid) and DCT (a taxane) impact negatively on the structural integrity and function of the rabbit OS at post-exposure day 10. These drugs, which disrupt microtubules through different mechanisms, cause reduction in thickness of the OM epithelium, diameter of ORN axon bundles, density of ORNs, cilia/ ORN, volumes and linear dimensions of the OB and OBCs, and olfactory sensitivity, with the reduction in all the aforementioned parameters being greater in DCT than in VBS-treated animals. Plausibly, these data may form an important basis for more informed use of MTTDs (i.e. vinca alkaloids and taxanes) in the management of patients with cancer. Future studies should compare the long-term effects of repeated doses of MTTDs on the OS across a wider variety of drugs and explore the molecular mechanisms underlying their differential potential to induce lesions in the nervous system.

Acknowledgement

The authors thank technical staff in the Department of Veterinary Anatomy & Physiology (Messrs Robert Tsuma, John Kiai and Francis Okumu) and in the Department of Human Anatomy and Medical Physiology, University of Nairobi, for their excellent technical assistance. Part of this work received support from the University of Nairobi (Grant No. 500-655-640).

References

1. Doucet S, Soussignan R, Sagot P, Schaal B. The secretion of areolar (Montgomery's) glands from lactating women elicits selective, unconditional responses in neonates. *PLoS One* 2009;4:e75792
2. Havlicek J, Roberts SC. MHC-correlated mate choice in humans: a review. *Psychoneuroendocrinology* 2009; 34:497-512.
3. Stevenson RJ. An initial evaluation of the functions of human olfaction. *Chem Senses* 2010;35:3-20
4. Kavoi BM, Makanya AN, Johanna P, Kiama SG. Morphofunctional adaptations of the olfactory mucosa in postnatally developing rabbits. *Anat Rec (Hoboken)* 2012; 295:1352-13635
5. Le Bon AM, Datiche F, Gascuel J, Grosmaître X. Olfactory system

- in mammals: structural and functional anatomy. *Flavour: From Food to Perception*; 2016:1-33.
6. Onyono PN, Kavoi BM, Kiama SG, Makanya AN. Functional morphology of the olfactory mucosa and olfactory bulb in fossorial rodents: The East African root rat (*Tachyoryctes splendens*) and the naked mole rat (*Heterocephalus glaber*). *Tissue Cell* 2017; 49:612-621.
 7. Buck L, Axel R. A novel multigene family may encode odorant receptors: A molecular basis for odor recognition. *Cell* 1991;65:175-187
 8. Menco BP, Cunningham AM, Qasba P, Levy N, Reed RR. Putative odour receptors localize in cilia of olfactory receptor cells in rat and mouse: a freeze substitution ultrastructural study. *J Neurocytol* 1997; 26:691-706.
 9. Pinto JM. Olfaction. *Proceedings of the American Thoracic Society*. March 1, 2011;8:46-52.
 10. Imamura F, Ito A, LaFever BJ. Subpopulations of projection neurons in the olfactory bulb. *Front Neural Circuits* 2020; 14:561822.
 11. Price JL. Olfaction. In: Paxinos G, Mai JM, eds. *The Human Nervous System*. 2nd ed. San Diego: Elsevier; 2004: 1198-1212
 12. Linster C, Cleland TA. Glomerular microcircuits in the olfactory bulb. *Neural Netw* 2009; 22: 1169-1173
 13. Brann JH, Firestein SJ. A lifetime of neurogenesis in the olfactory system. *Front Neurosci* 2014; 8:182
 14. Kikuta S, Nagayama S, Hasegawa-Ishii S. Structures and functions of the normal and injured human olfactory epithelium. *Front Neural Circuits* 2024;18:1406218.
 15. Wang L, Liu SY, Zheng HY, Fang SM, *et al.* Olfactory dysfunction induced by pesticides: Adverse outcomes, emerging mechanisms, and risk for neurodegenerative diseases. *Pestic Biochem Physiol* 2025; 106474
 16. LaFever BJ, Imamura F. Effects of nasal inflammation on the olfactory bulb. *J Neuroinflammation* 2022; 19:294.
 17. Rantala JK, Edgren H, Lehtinen L, *et al.* Integrative functional genomics analysis of sustained polyploidy phenotypes in breast cancer cells identifies an oncogenic profile for GINS2. *Neoplasia* 2010; 12:877-IN14.
 18. Remesh A. Toxicities of anticancer drugs and its management. *Int J Basic Clin Pharmacol* 2012; 1: 2-12
 19. Awadallah N, Proctor K, Joseph KB, Delay ER, Delay RJ. Cyclophosphamide has long-term effects on proliferation in olfactory epithelia. *Chem Senses* 2020; 45:97-109.
 20. Was H, Borkowska A, Bagues A, *et al.* Mechanisms of chemotherapy-induced neurotoxicity. *Front Pharmacol* 2022; 13:750507.
 21. Krause W. Resistance to anti-tubulin agents: From vinca alkaloids to eopothilones. *Cancer Drug Resist* 2019;2:82-106
 22. Zhang D, Kanakkhanthara A. Beyond the paclitaxel and vinca alkaloids: Next generation of plant-derived microtubule-targeting agents with potential anticancer activity. *Cancers* 2020;12:1721.
 23. Janke C, Bulinski J. Post-translational regulation of the microtubule cytoskeleton: mechanisms and functions. *Nat Rev Mol Cell Biol* 2011;12:773-786.
 24. Topp KS, Tanner KD, Levine JD. Damage to the cytoskeleton of large diameter sensory neurons and myelinated axons in vincristine-induced painful peripheral neuropathy in the rat. *J Comp Neurol* 2000; 424:563-576.
 25. Correia JJ, Lobert S. Physiochemical aspects of tubulin-interacting antimetabolic drugs. *Curr Pharm Des* 2001;7:1213-1228.
 26. Moudi M, Go R, Seok Yien CY, Nazre M. Vinca alkaloids. *Int J Prev Med* 2013;4:1231.
 27. Parness J, Horwitz SB. Taxol binds to polymerized tubulin in vitro. *J Cell Biol* 1981;91:479-487.
 28. Galsky MD, Dritselis A, Kirkpatrick P, Oh WK. Cabazitaxel. *Nat Rev Drug Discov* 2010;9:677-678.
 29. Todd GC, Gibson WR, Morton DM. Toxicology of vindesine (desacetyl vinblastine amide) in mice, rats, and dogs. *J Toxicol Environ Health A* 1976; 1:843-849.
 30. Kanter PM, Klaich GM, Bullard GA, King JM, Bally MB, Mayer LD. Liposome encapsulated vincristine: preclinical toxicologic and pharmacologic comparison with free vincristine and empty liposomes in mice, rats and dogs. *Anticancer Drugs* 1994;5:579-590.
 31. Dorr RT, Alberts DS. Vinca alkaloid skin toxicity: antidote and drug disposition studies in the mouse. *J Natl Cancer Inst* 1985;74:113-120.
 32. Kai K, Satoh H, Kashimoto Y, Kajimura T, Furuhashi K. Olfactory epithelium as a novel toxic target following an intravenous administration of vincristine to mice. *Toxicol Pathol* 2002;30:306-311.
 33. Kai K, Satoh H, Kajimura T, *et al.* Olfactory epithelial lesions induced by various cancer chemotherapeutic agents in mice. *Toxicol Pathol* 2004;32:701-709.
 34. Kai K, Yoshida M, Sugawara, Kato M, Furuhashi K. Investigation of apoptosis in the murine olfactory epithelium evoked by vincristine sulphate in comparison with that induced by unilateral bulbectomy. The 24th Society of Toxicologic Pathology Annual meeting; 2005; Washington, DC.
 35. Kai K, Sahto H, Yoshida M, *et al.* Species and sex differences in susceptibility to olfactory lesions among the mouse, rat and monkey following an intravenous injection of vincristine sulphate. *Toxicol Pathol* 2006; 34:223-231.
 36. Kavoi BM, Makanya AN, Kiama SG. Anticancer drug vinblastine sulphate induces transient morphological changes on the olfactory mucosa of the rabbit. *Anat Histol Embryol* 2012;41:374-387.
 37. Kavoi BM, Plendl J, Makanya AN, Kiama SG. Effects of anticancer drug docetaxel on the structure and function of the rabbit olfactory mucosa. *Tissue Cell* 2014;46:213-224.
 38. Hochadel M. *Mosby's Drug Reference for Health Professions*. 3rd ed. USA: Mosby; 2011.
 39. Bang YJ, Kang WK, Kang YK, *et al.* Docetaxel 75 mg/m² is active and well tolerated in patients with metastatic or recurrent gastric cancer: a phase II trial. *Jpn J Clin Oncol* 2002;32:248-254.
 40. Reagan-Shaw S, Nihal M, Ahmad N. Dose translation from animal to human studies revisited. *FASEB J* 2008; 22:659-561.
 41. Kavoi, B., Makanya, A., Hassanali, J., Carlsson, H.E. and Kiama, S., 2010. Comparative functional structure of the olfactory mucosa in the domestic dog and sheep. *Annals of Anatomy-Anatomischer Anzeiger*, 192(5), pp.329-337 Kavoi B, Makanya A, Hassanali J, Carlsson HE, Kiama S. Comparative functional structure of the olfactory mucosa in the domestic dog and sheep. *Ann Anat* 2010;192:329-337.
 42. Ibe CS, Salami SO, Wanmi N. Brain size of the African grasscutter (*Thryonomys swinderianus*, Temminck, 1827) at defined postnatal periods. *Folia Vet* 2017; 61:5-11.
 43. Alers JC, Krijtenburg PJ, Vissers KJ, van Dekken H. Effect of bone decalcification procedures on DNA in situ hybridization and comparative genomic hybridization: EDTA is highly preferable to a routinely used acid decalcifier. *J Histochem Cytochem* 1999;47:703-709.
 44. Kavoi BM, Ochieng' SJ. Histology and ultrastructure of olfactory and nasal respiratory mucosae in suckling and adult African grasscutters (*Thryonomys swinderianus*-Temminck, 1827). *Zoomorphology* 2023; 142:215-23.
 45. Kavoi BM, Kisipan ML. A Gross morphometric study of olfactory brain components in the Rufous sengi (*Elephantulus rufescens*). *Int J Morphol* 2019; 37: 1003-1007
 46. Scherle W. A simple method for volumetry of organs in quantitative stereology. *Mikroskopie* 1970; 26:57-60
 47. Nathan BP, Yost J, Litherland MT, Struble RG, Switzer PV. Olfactory function in apoE knockout mice. *Behav Brain Res* 2004;150:1-7.
 48. Dawson PA, Steane SE, Markovich D. Impaired memory and olfactory performance in NaSi-1 sulphate transporter deficient mice. *Behav Brain Res* 2005;159:15-20.
 49. Yang M, Crawley JN. Simple behavioral assessment of mouse olfaction. *Curr Protoc Neurosci* 2009; 48:8-24
 50. Chirino R, Beyer C, González-Mariscal G. Lesion of the main olfactory epithelium facilitates maternal behavior in virgin rabbits. *Behav Brain Res* 2007;180:127-132.
 51. Rosati, D., Mastino, P., Romeo, M., de Soccio, G., Pentangelo, D., Petrella, C., Barbato, C. and Minni, A., 2024. Taste and smell

- alterations (TSAs) in cancer patients. *Diseases*, 12(6), p.130 Rosati D, Mastino P, Romeo M, *et al.* Taste and smell alterations (TSAs) in cancer patients. *Diseases* 2024; 12:130.
52. Riga M, Chelis L, Papazi T, Danielides V, Katotomichelakis M, Kakolyris S. Hyposmia: an underestimated and frequent adverse effect of chemotherapy. *Support Care Cancer* 2015; 23:3053-3058.
53. Ijpma I, Renken RJ, Gietema JA, *et al.* Changes in taste and smell function, dietary intake, food preference, and body composition in testicular cancer patients treated with cisplatin-based chemotherapy. *Clin Nutr* 2017; 36:1642-1648.
54. Alonzi S, Hoerger M, Perry LM, *et al.* Changes in taste and smell of food during prostate cancer treatment. *Support Care Cancer* 2021; 29:2807-2809.
55. Webber TB, Briata IM, DeCensi A, Cevasco I, Paleari L. Taste and Smell Disorders in Cancer Treatment: Results from an Integrative Rapid Systematic Review. *Int J Mol Sci* 2023; 24:2538.
56. Jacobs DI, Snoeijer W, Hallard D, Verpoorte R. The Catharanthus alkaloids: pharmacognosy and biotechnology. *Curr Med Chem* 2004; 11:607-628.
57. Arora RD, Menezes RG. *Vinca Alkaloid Toxicity*. Treasure Island: StatPearls Publishing; 2021
58. Banyal A, Tiwari S, Sharma A, *et al.* Vinca alkaloids as a potential cancer therapeutics: recent update and future challenges. *Biotech* 2023; 13:211.
59. Adams JD, Flora KP, Goldspiel BR, Wilson JW, Arbusk SG, Finley R. Taxol: a history of pharmaceutical development and current pharmaceutical concerns. *J Natl Cancer Inst Monogr* 1993; (15):141-147.
60. Škubník J, Pavlíčková V, Ruml T, Rimpelová S. Current perspectives on taxanes: Focus on their bioactivity, delivery and combination therapy. *Plants* 2021; 10:569.
61. Sousa-Pimenta, M., Estevinho, L.M., Szopa, A., Basit, M., Khan, K., Armaghan, M., Ibrayeva, M., Sönmez Güreç, E., Calina, D., Hano, C. and Sharifi-Rad, J., 2023. Chemotherapeutic properties and side-effects associated with the clinical practice of terpene alkaloids: paclitaxel, docetaxel, and cabazitaxel. *Frontiers in pharmacology*, 14, p.1157306
62. Sokolowski K, Turner PV, Lewis E, Wange RL, Fortin MC. Exploring rabbit as a nonrodent species for general toxicology studies. *Toxicol Sci* 2024; 199:29-39.
63. Calof AL, Hagiwara N, Holcomb JD, Mumm JS, Shou J. Neurogenesis and cell death in olfactory epithelium. *J Neurobiol* 1996; 30:67-81.
64. Langlois MJ, Bergeron S, Bernatchez G, *et al.* The PTEN phosphatase controls intestinal epithelial cell polarity and barrier function: role in colorectal cancer progression. *PLoS One* 2010; 5:e15742.
65. Jenkins PM, McEwen DP, Martens JR. Olfactory cilia: linking sensory cilia function and human disease. *Chem Senses* 2009; 34:451-464.

Mini Curriculum and Author's Contribution

1. Boniface Mwanzia Kavoi - BVM, MSc, PhD. Contribution: Was involved in all steps of this study including its conception, design, material preparation, data collection and analysis and writing of the manuscript. ORCID: 0000-0001-7526-1158.

Received: July 10, 2025
Accepted: October 10, 2025

Corresponding author
Boniface Mwanzia Kavoi
E-mail: bmkavoi@uonbi.ac.ke/ drkanvo@yahoo.com